

Self-Consistent Collective Motion Path for Nuclear Fusion/Fission Reactions

Kai Wen and Takashi Nakatsukasa

Center for Computational Sciences, University of Tsukuba, Tsukuba 305-8577, Japan

Abstract

The adiabatic self-consistent collective coordinate (ASCC) method is a microscopic theoretical framework to extract an optimal form of collective coordinate for the large amplitude nuclear collective motion. It also enables us to calculate the inertial mass for the nuclear collective motion. Based on this theoretical framework, we develop a numerical method to realize a calculation of the self-consistent collective motion path and inertial mass parameter for the nuclear fusion/fission reactions. We apply our method to the reaction ${}^8\text{Be} \leftrightarrow \alpha + \alpha$. The collective motion paths, collective potentials, and inertial masses for the relative motion are presented and discussed.

Keywords: *Nuclear fission; collective motion; collective path*

1 Introduction

The time-dependent density functional theory (TDDFT) [1–5] is a general microscopic theoretical framework to study low-energy nuclear fusion and fission reactions. Based on the TDDFT, a microscopic mechanism of nuclear collective dynamics has been extensively studied for many years. The linear approximation of TDDFT leads to the random-phase approximation (RPA) [5–7], which is capable of nuclear response calculations and provides an unified description for both the nuclear structure and collective dynamics. Despite a rich microscopic information embedded in the TDDFT calculations, it is difficult to give a full theoretical description for the nuclear collective dynamics. For instance, it cannot describe the sub-barrier fusion and spontaneous fission properly, due to its semiclassical nature [1, 5, 6].

For the study of large amplitude nuclear collective dynamics in the “macroscopic” collective level, it is of high interest to obtain an optimal form of collective variables maximally decoupled from other intrinsic degrees of freedom, so that equations of motion for these collective canonical variables become of closed form. The adiabatic self-consistent collective coordinate (ASCC) method [8–11] aims at determining such canonical variables by solving self-consistent equations. The ASCC method has been applied to many nuclear structure problems associated with large-amplitude oscillations described by Hamiltonians with separable interactions [10–13].

Proceedings of the International Conference ‘Nuclear Theory in the Supercomputing Era — 2016’ (NTSE-2016), Khabarovsk, Russia, September 19–23, 2016. Eds. A. M. Shirokov and A. I. Mazur. Pacific National University, Khabarovsk, Russia, 2018, p. 115.

<http://www.ntse-2016.khb.ru/Proc/Wen.pdf>.

The inertial mass of nuclear collective motion is another long-standing problem in nuclear structure physics [6, 14]. Apparently, it is very important for nuclear reaction dynamics. Especially, the derivation of the mass after a touch of two nuclei is a highly non-trivial problem. The calculation of the mass parameter requires properly extracted collective coordinates and conjugate momenta, which can be provided by the ASCC method. Thus the ASCC method is also capable of microscopic calculation of the inertial masses for the collective motion.

Recently, by combining the imaginary-time evolution [15] and the finite amplitude method [16–18], we proposed a numerical method to solve the ASCC equations and to determine a collective path for the nuclear collective motion [19]. The collective coordinate and momentum are obtained self-consistently. In this article we will introduce our method and present the first applications to simplest systems, the translational motion of a single alpha particle and the fission of ${}^8\text{Be}$.

In Section 2, we give the formulation of the basic ASCC equations in the case of one-dimensional collective motion, introduce the method of constructing the collective path and the coordinate transformation procedure for calculating the mass parameter. In Section 3, we apply the method to the translational motion of a single alpha particle and to the reaction ${}^8\text{Be} \leftrightarrow \alpha + \alpha$. Summary and concluding remarks are given in Section 4.

2 Formulation of the ASCC method

To determine an optimal collective path in the high-dimensional space of Slater determinants, we first label the states on the collective path by a couple of canonical variables (p, q) , whose equation of motion can be maximally decoupled from other intrinsic degrees of freedom. Thus q and p represent the collective coordinate and the conjugate momentum respectively.

In the adiabatic limit, expanding the wave function $\psi(q, p)$ in powers of p up to the second order, the invariance principle of the SCC equation [8] leads to the equations of the ASCC method [5, 9]. Neglecting the curvature terms, it reduces to the following set of equations:

$$\delta\langle\Psi(q)|\hat{H}_{\text{mv}}|\Psi(q)\rangle = 0, \quad (1)$$

$$\delta\langle\Psi(q)|[\hat{H}_{\text{mv}}, \frac{1}{i}\hat{P}(q)] - \frac{\partial^2 V(q)}{\partial q^2}\hat{Q}(q)|\Psi(q)\rangle = 0, \quad (2)$$

$$\delta\langle\Psi(q)|[\hat{H}_{\text{mv}}, i\hat{Q}(q)] - \frac{1}{M(q)}\hat{P}(q)|\Psi(q)\rangle = 0, \quad (3)$$

with the moving mean-field Hamiltonian \hat{H}_{mv} defined as

$$\hat{H}_{\text{mv}} = \hat{H} - \frac{\partial V(q)}{\partial q}\hat{Q}(q), \quad (4)$$

where the potential $V(q)$ is the expectation value of the Hamiltonian,

$$V(q) = \langle\psi(q)|\hat{H}|\psi(q)\rangle, \quad (5)$$

$M(q)$ is the mass parameter of collective motion. $\hat{Q}(q)$ and $\hat{P}(q)$ correspond to the local generators of the variables p and q . Note that the collective motion path is

expressed by $\Psi(q)$, which represents the state $\Psi(q, p)$ with $p = 0$. Here we consider the one-dimensional description of collective motion without taking the pairing correlation into account. Equation (1) is similar to a constrained Hartree–Fock (HF) problem, however, the constraint operator $\hat{Q}(q)$ depends on the coordinate q , which is self-consistently determined by the RPA-like Eqs. (2) and (3) called moving RPA equations. The conventional RPA forward and backward amplitudes X and Y are linear combinations of $\hat{P}(q)$ and $\hat{Q}(q)$ which matrix elements X_{ni} , Y_{ni} and P_{ni} , Q_{ni} satisfy the relations

$$X_{nj} = \sqrt{\frac{\omega}{2}} Q_{nj} + \frac{1}{\sqrt{2\omega}} P_{nj}, \quad (6)$$

$$Y_{nj} = \sqrt{\frac{\omega}{2}} Q_{nj} - \frac{1}{\sqrt{2\omega}} P_{nj}. \quad (7)$$

Hereafter, indices i, j and n, m refer to the hole and particle states respectively. The RPA eigenfrequency ω is related to the mass parameter and the second derivative of the potential,

$$\omega^2 = \frac{1}{M(q)} \frac{\partial^2 V(q)}{\partial q^2}. \quad (8)$$

The operators of collective momentum $\hat{P}(q)$ and coordinate $\hat{Q}(q)$, as a pair of canonical variables, are imposed a weak canonicity condition,

$$\langle \Psi(q) | [i\hat{P}(q), \hat{Q}(q)] | \Psi(q) \rangle = 1, \quad (9)$$

which is equivalent to the RPA normalization condition,

$$\sum_{n,j} (X_{nj}^2 - Y_{nj}^2) = 1. \quad (10)$$

The collective path $\Psi(q)$ as well as $V(q)$ and $M(q)$ are determined self-consistently by Eqs. (1)–(3) and no *a priori* assumption is used.

The scale of the collective coordinate q in the ASCC equation set is arbitrary. It is easy to determine the scale by mapping the coordinate q onto any other collective quantity R as far as the one-to-one correspondence exists. For the study of nuclear scattering and nuclear fission, we define R as the relative distance between ions. The operator form of R can be expressed as

$$\hat{R} \equiv \int d\vec{r} \hat{\psi}^\dagger(\vec{r}) \hat{\psi}(\vec{r}) z \left[\frac{\theta(z - z_s)}{M_{\text{pro}}} - \frac{\theta(z_s - z)}{M_{\text{tar}}} \right], \quad (11)$$

where θ is the step function, and z_s is an artificially introduced section plane dividing the total system of mass $A = M_{\text{pro}} + M_{\text{tar}}$ into the left part with mass M_{pro} and the right part with mass M_{tar} . The relation between $M(R)$ and $M(q)$ reads

$$M(R) = M(q) \left(\frac{dq}{dR} \right)^2. \quad (12)$$

The calculation of the derivative dq/dR is straightforward once the collective path $\Psi(q)$ and the local generator $\hat{P}(q)$ are obtained. With this equation we can calculate the mass parameter with respect to R .

We solve the moving RPA equations (2) and (3) by taking advantage of the finite amplitude method (FAM) [16–18], especially of the matrix FAM prescription [18]. To solve the ASCC equations (1)–(3) self-consistently and to construct the collective motion path $\Psi(q)$, we adopt the following procedures: First, we calculate the HF ground state of the nucleus before fission $\Psi(q = 0)$; based on $\Psi(q = 0)$, we solve the moving RPA equations to obtain $\hat{Q}(q = 0)$ and $\hat{P}(q = 0)$. When $\Psi(q)$, $\hat{Q}(q)$, and $\hat{P}(q)$ are provided, we solve the moving HF equation to obtain the state $\Psi(q + \delta q)$ by using the constraint condition

$$\langle \Psi(q + \delta q) | \hat{Q}(q) | \Psi(q + \delta q) \rangle = \delta q. \quad (13)$$

With the new state $\Psi(q + \delta q)$, we may update the generators and get $\hat{Q}(q + \delta q)$ and $\hat{P}(q + \delta q)$; with the updated generators, we can obtain the new state by Eq. (13) again. Carrying on this iterative procedure, we can determine series of states $\Psi(0)$, $\Psi(\delta q)$, $\Psi(2\delta q)$, $\Psi(2\delta q)$, ... and obtain the ASCC collective path. The assumption adopted here is that $\Psi(q + \delta q) \simeq e^{-i\delta q \hat{P}(q)} \Psi(q)$.

3 Applications

3.1 Solution for the translational motion

The HF ground state is a trivial solution that satisfies the ASCC equations. Based on the ground state, we can calculate the translational mass as a test calculation. The calculation is done in the 3-dimensional coordinate space in a sphere with radius equal to 7 fm. The BKN energy density functional [20] is adopted in numerical calculation. The upper panel in Fig. 1 shows the eigenfrequency ω of several lowest RPA states for the ground state of alpha particle. Three translational modes along x , y , z axes are degenerate with an energy of about 1 MeV. The model space is discretized with the mesh size of 0.8 fm. Using a finer mesh size, the eigenfrequencies of these three modes approaches to zero. Due to a compact nature of alpha particle, the lowest physical excited state above the translational zero-modes, is 20 MeV higher representing a monopole vibration.

Below those three degenerated translational modes, there exists a mode with the energy equal to zero, this solution appears due to a numerical treatment of the particle states, namely, the particle state $|m\rangle$ is expressed through the coordinate $|\vec{r}\rangle$ in the whole model space. This redundancy in the representation of particle states results in additional solutions that are unphysical. This unphysical state does not affect the physical results and we may simply neglect it. Using Eq. (12), we calculate the translational mass parameter of the alpha particle. The model space is chosen to be a sphere with different mesh sizes. The lower panel in Fig. 1 shows the mass parameters of alpha particle in the translational motion along x , y and z axes and their dependence on the mesh size. As the mesh size decrease, the results approach the value of 4 in the units of nucleon mass, which is the correct mass number of the alpha particle.

3.2 ASCC motion path for ${}^8\text{Be} \leftrightarrow \alpha + \alpha$

A numerical application of the ASCC method to establishing a collective path for the nuclear fusion or fission reactions is a complicated computational problem. We

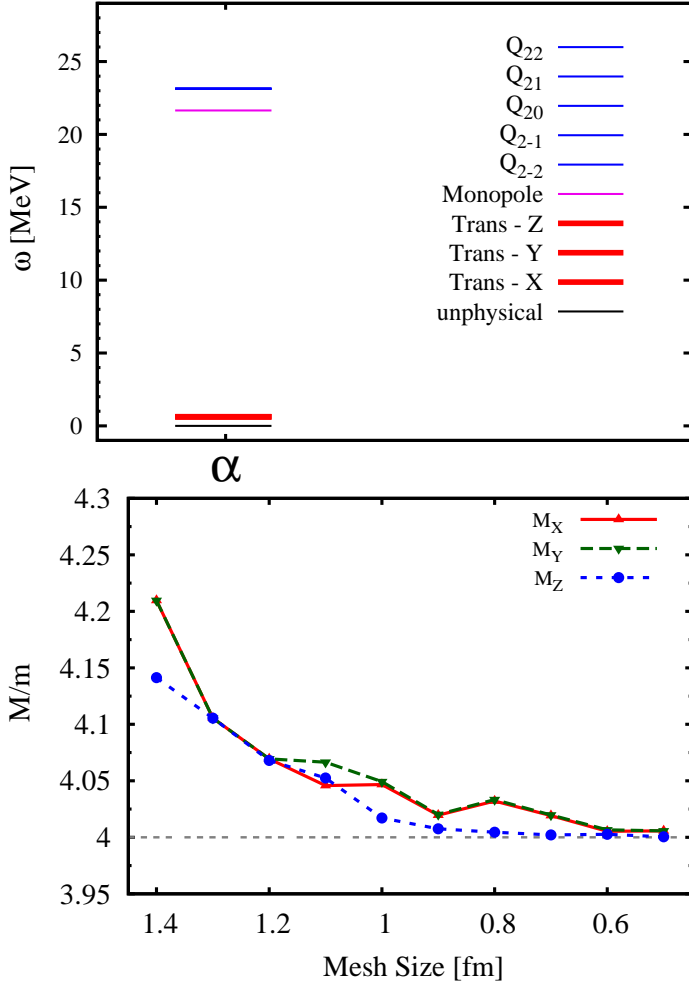


Figure 1: Top: calculated eigenfrequencies for the ground state of alpha particle. Three translational motion modes along x , y and z axis are shown by thick red lines. These three translational modes are degenerate, five quadrupole modes are also degenerate. Bottom: calculated translational mass of the alpha particle in units of nucleon's mass as a function of the mesh size.

show here our first result for the spontaneous fission path of ${}^8\text{Be}$, that may be also regarded as the fusion path of two alpha particles at low incident energy. The model space is the three-dimensional grid space of the rectangular box size $10 \times 10 \times 18 \text{ fm}^3$ with the mesh size of 0.8 fm . The BKN energy density functional [20] is adopted in numerical calculation.

Starting from the ground state of ${}^8\text{Be}$ and carrying out the iterative procedure introduced in Section 2, we obtain the ASCC fission path of ${}^8\text{Be}$ demonstrating a smooth transformation of ${}^8\text{Be}$ into two well separated alpha particles. In Fig. 2, we show the calculated density distribution at four points on this collective path. The inset (a) shows the density distribution of the ground state of ${}^8\text{Be}$ at $R = 3.55 \text{ fm}$ while the inset (d) shows the density distribution of two alpha particles at $R = 6.40 \text{ fm}$. The insets (b) and (c) show the intermediate density distributions at $R = 4.10 \text{ fm}$ and 5.10 fm , respectively.

In the upper panel of Fig. 3, we plot the frequency ω of Eq. (8) for the solution of the moving RPA equations on the ASCC path compared with the binding energy of the last filled orbit as a function of R . The lower panel of Fig. 3 shows the potential

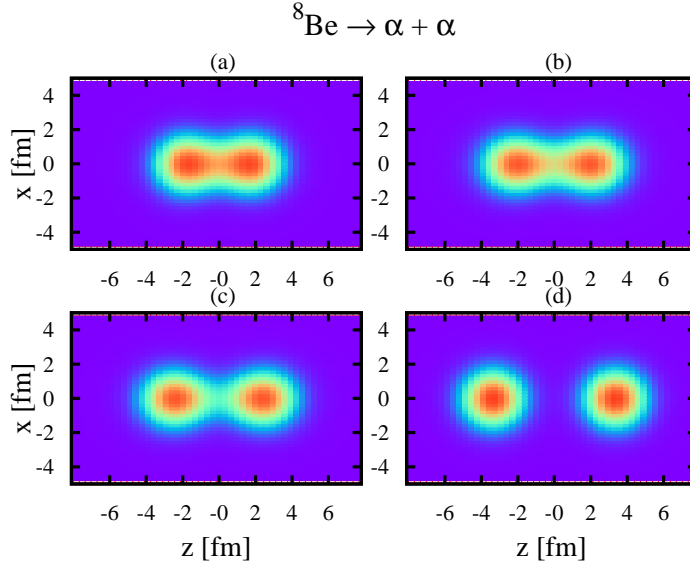


Figure 2: Calculated density distribution at four points on the ASCC collective fission path of ${}^8\text{Be}$. Insets (a), (b), (c), and (d) show the density distribution in the $y-z$ plane of the ground state of ${}^8\text{Be}$ at $R = 3.55, 4.10, 5.10$, and 6.40 fm, respectively.

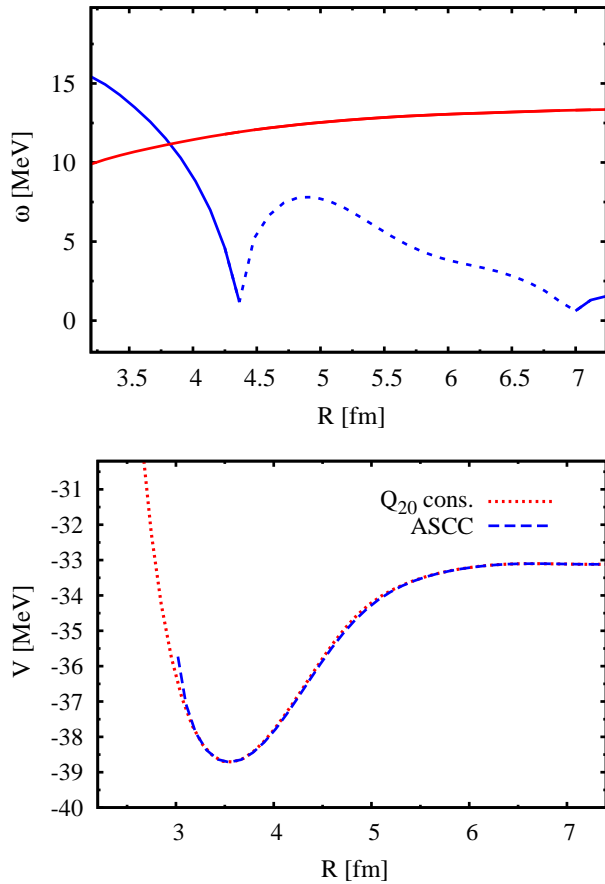


Figure 3: Top: RPA eigenfrequency ω on the ASCC collective fission path of ${}^8\text{Be}$ as a function of R . Solid (dashed) blue curve shows real (imaginary) ω , red curve demonstrates an absolute value of the single particle energy of the last filled orbit in ${}^8\text{Be}$. Bottom: potential energy as a function of R . Blue curve presents the potential on the ASCC collective path while the red curve is the potential of the constrained HF states with the constraint on Q_{20} .

energy as a function of R . The ground state of ${}^8\text{Be}$ is at $R = 3.55$ fm, the Coulomb barrier top is at $R = 6.6$ fm.

According to Eq. (8), ω^2 is proportional to the second order derivative of the collective potential $V(q)$ which can be negative. In the upper panel of Fig. 3, the imaginary ω is plotted by the dashed curve while the real one is plotted by the solid curve. In the region $4.4 \text{ fm} < R < 6.9 \text{ fm}$, the imaginary ω appears, where the state is not in the minimum but on the saddle point of the energy surface corresponding to the moving Hamiltonian H_{mv} . At a larger distance, ω should approach zero. As a general trend, the frequency ω for the relative motion increases as the nuclei approach each other. Inside the HF ground state at $R < 3.6$ fm, ω increases drastically and becomes larger than the binding energy of the last filled orbit, the RPA excitation here is above the bound threshold and in the continuum region. In this case the unbound RPA state features depend on the choice of model space, therefore we should not take the result in this region seriously.

3.3 Inertial mass for ${}^8\text{Be} \leftrightarrow \alpha + \alpha$

With the collective fission path obtained, the ASCC inertial mass $M_{\text{ASCC}}(R)$ for this fission path is calculated using Eq. (12) and shown in Fig. 4 in comparison with the cranking mass $M_{\text{cr}}(R)$.

The cranking inertial mass is derived by assuming a separable interaction and taking the adiabatic limit of the RPA inertial mass. In the case of one-dimensional motion, the widely used formula for the cranking mass reads [21]

$$M_{\text{cr}}(R) = \frac{1}{2} \left\{ S^{(1)}(R) \right\}^{-1} S^{(3)}(R) \left\{ S^{(1)}(R) \right\}^{-1}, \quad (14)$$

where

$$S^{(k)}(R) = \sum_{m,i} \frac{|\langle \varphi_m(R) | \hat{R} | \varphi_i(R) \rangle|^2}{\{e_m(R) - e_i(R)\}^k}. \quad (15)$$

Here the single-particle states $\phi(R)$ and energies $e(R)$ are defined with respect

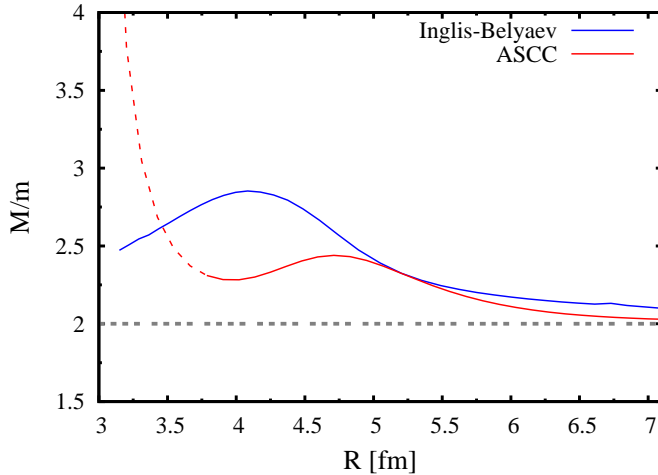


Figure 4: Inertial mass for the fission path of ${}^8\text{Be}$ as a function of relative distance R in the units of nucleon mass. Red (blue) curve is the ASCC (cranking) mass, the cranking mass is obtained with the CHF states with the constraint on R .

to $h_{\text{CHF}}(R) = h_{\text{HF}}[\rho] - \lambda(R)\hat{R}$ as

$$h_{\text{CHF}}(R)\varphi_\mu(R) = e_\mu(R)\varphi_\mu(R), \quad \mu = i, m. \quad (16)$$

Residual fields induced by the density fluctuations are neglected in the cranking formula. The calculation of the cranking mass is based on the CHF states with the constraint on R . The model space is the same as that for the ASCC.

As is seen in Fig. 4, the ASCC mass $M_{\text{ASCC}}(R)$ is smaller than the cranking mass. At large distance, both produce the reduced mass of 2 in the units of nucleon mass, which is just the reduced mass for the relative motion of two alpha particles; the precision of cranking mass is a little worse as compared with the ASCC mass. In the interior region after the touch of two nuclei, these masses have very different values. The cranking mass is found to be larger than the ASCC mass, especially at around $R = 4$ fm, the cranking mass has an about 40 percent larger value. This fact shows that the residual field arising from the density fluctuations makes a significant contribution. Compared with the cranking mass, the ASCC mass has an advantage that the collective coordinate as well as the wave functions are not assumed artificially but calculated self-consistently. As mentioned in the previous Subsection, we should not take seriously the results for the ASCC mass at $R < 3.6$ fm, the ASCC mass is plotted in this region by a dashed curve.

4 Summary

Based on the ASCC theory, we presented a method to determine the collective motion path for the large amplitude nuclear collective motion, and applied this method to the nuclear fusion/fission reaction ${}^8\text{Be} \leftrightarrow \alpha + \alpha$. In the 3D coordinate space representation, the reaction path, the collective potential and the inertial mass are calculated. Since the system under consideration presents one of the simplest cases, there is no significant difference in the reaction path as compared with that for the CHF states. The ASCC collective potential is similar to the potential of the CHF states. A comparison of the ASCC mass with the cranking mass is presented. The ASCC mass improves the cranking mass by taking into account the residual interaction caused by the density fluctuations. By using this method it is feasible to calculate the mass parameter for any collective coordinate. As our first application, we use a schematic BKN interaction, it is desired to use more realistic interactions accounting for paring in our future study.

References

- [1] J. W. Negele, Rev. Mod. Phys. **54**, 913 (1982).
- [2] C. Simenel, Eur. Phys. J. A **48**, 1 (2012).
- [3] T. Nakatsukasa, Progr. Theor. Exp. Phys. **2012**, 01A207 (2012).
- [4] J. A. Maruhn, P.-G. Reinhard, P. D. Stevenson and A. S. Umar, Comput. Phys. Commun. **185**, 2195 (2014).
- [5] T. Nakatsukasa, K. Matsuyanagi, M. Matsuo and K. Yabana, Rev. Mod. Phys. **88**, 045004 (2016).

- [6] P. Ring and P. Schuck, *The nuclear many-body problem*. Springer-Verlag, Berlin, Heidelberg, 1980.
- [7] J.-P. Blaizot and G. Ripka, *Quantum theory of finite systems*. MIT Press, Cambridge, 1986.
- [8] T. Marumori, T. Maskawa, F. Sakata and A. Kuriyama, Progr. Theor. Phys. **64**, 1294 (1980).
- [9] M. Matsuo, T. Nakatsukasa and K. Matsuyanagi, Progr. Theor. Phys. **103**, 959 (2000).
- [10] N. Hinohara, T. Nakatsukasa, M. Matsuo and K. Matsuyanagi, Progr. Theor. Phys. **117**, 451 (2007).
- [11] N. Hinohara, T. Nakatsukasa, M. Matsuo and K. Matsuyanagi, Phys. Rev. C **80**, 014305 (2009).
- [12] N. Hinohara, Z. P. Li, T. Nakatsukasa, T. Nikšić and D. Vretenar, Phys. Rev. C **85**, 024323 (2012).
- [13] K. Sato, N. Hinohara, K. Yoshida, T. Nakatsukasa, M. Matsuo and K. Matsuyanagi, Phys. Rev. C **86**, 024316 (2012).
- [14] A. Bohr and B. R. Mottelson, *Nuclear structure. Vol. 2*. Benjamin, New York, 1975.
- [15] K. T. R. Davies, H. Flocard, S. Krieger and M. S. Weiss, Nucl. Phys. A **342**, 111 (1980).
- [16] T. Nakatsukasa, T. Inakura and K. Yabana, Phys. Rev. C **76**, 024318 (2007).
- [17] P. Avogadro and T. Nakatsukasa, Phys. Rev. C **84**, 014314 (2011).
- [18] P. Avogadro and T. Nakatsukasa, Phys. Rev. C **87**, 014331 (2013). C **76**, 024318 (2007).
- [19] K. Wen and T. Nakatsukasa, Phys. Rev. C **96**, 014610 (2017).
- [20] P. Bonche, S. Koonin and J. W. Negele, Phys. Rev. C **13**, 1226 (1976).
- [21] A. Baran, J. A. Sheikh, J. Dobaczewski, W. Nazarewicz and A. Staszczak, Phys. Rev. C **84**, 054321 (2011).